Development 138, 2705-2715 (2011) doi:10.1242/dev.060277

Fibroblast growth factor signalling controls successive cell behaviours during mesoderm layer formation in *Drosophila*

Ivan B. N. Clark[1], Villö Muha[1], Anna Klingseisen[1], Maria Leptin[2] and Hans-Arno J. Müller[1,*]

SUMMARY

Fibroblast growth factor (FGF)-dependent epithelial-mesenchymal transitions and cell migration contribute to the establishment of germ layers in vertebrates and other animals, but a comprehensive demonstration of the cellular activities that FGF controls to mediate these events has not been provided for any system. The establishment of the *Drosophila* mesoderm layer from an epithelial primordium involves a transition to a mesenchymal state and the dispersal of cells away from the site of internalisation in a FGF-dependent fashion. We show here that FGF plays multiple roles at successive stages of mesoderm morphogenesis in *Drosophila*. It is first required for the mesoderm primordium to lose its epithelial polarity. An intimate, FGF-dependent contact is established and maintained between the germ layers through mesoderm cell protrusions. These protrusions extend deep into the underlying ectoderm epithelium and are associated with high levels of E-cadherin at the germ layer interface. Finally, FGF directs distinct hitherto unrecognised and partially redundant protrusive behaviours during later mesoderm spreading. Cells first move radially towards the ectoderm, and then switch to a dorsally directed movement across its surface. We show that both movements are important for layer formation and present evidence suggesting that they are controlled by genetically distinct mechanisms.

KEY WORDS: Cell signalling, Gastrulation, Cell migration, E-cadherin, Fibroblast growth factor, *Drosophila*

INTRODUCTION

The development of tissues and organs depends on coordinated cell movements. Some tissues migrate as epithelial structures, maintaining apical-basal polarity, whereas others undergo a transition to a mesenchymal state (EMT) prior to migration (Biname et al., 2010). Mesenchymal cells migrate individually or as a collective, in which cells can move relative to each other while engaging and disengaging cell contacts (Weijer, 2009). It is not fully understood which cell behaviours contribute to collective migration and how intrinsic and extrinsic signals coordinate collective cell migration.

The formation of the mesoderm in *Drosophila* is a well-studied example of collective cell movement and we have extensive knowledge of its genetic regulation (Leptin, 1999). The mesoderm primordium invaginates and is internalised as an epithelial monolayer (Costa et al., 1993; Leptin and Grunewald, 1990). The cells then undergo EMT and establish a multilayered aggregate apposed to the basal surface of the neuroectoderm epithelium. This multi-layered mesoderm aggregate spreads out between the neuroectoderm and the centrally located yolk cell and eventually forms a transient monolayer (Fig. 1A,B). Mesoderm layer formation depends on signalling by the FGF8-like ligands Thisbe (Ths) and Pyramus (Pyr) through the FGF receptor Heartless (Htl) (Beiman et al., 1996; Gryzik and Müller, 2004). Htl is expressed in the mesoderm cells while the ligands exhibit a dynamic expression pattern in the neuroectoderm (Klingseisen et al., 2009; Shishido et al., 1993; Stathopoulos et al., 2004).

[1]Division of Cell and Developmental Biology, College of Life Sciences, University of Dundee, Dundee DD1 5EH, UK. [2]Institut für Genetik, Universität zu Köln, 50931 Cologne, Germany.

*Author for correspondence (h.j.muller@dundee.ac.uk)

Accepted 15 April 2011

FGF signalling is also implicated in mesoderm formation in vertebrate gastrulation. In mouse embryos, FGF signalling is required for EMT and ingression of epiblast cells to form the mesoderm layer (Ciruna and Rossant, 2001; Sun et al., 1999). One mechanism by which FGF signalling initiates EMT is through maintaining expression of Snail-family transcription factors, which downregulate epithelial gene networks (Nieto et al., 1994). In chick gastrulation, FGFs play an important role in directing the collective migration of the mesoderm cells after ingression, whereas their function in EMT in the primitive streak is less clear (Chuai and Weijer, 2009a).

During *Drosophila* mesoderm layer formation, cells at the dorsal edge of the mesoderm aggregate extend protrusions pointing in the direction of their migration (Schumacher et al., 2004). These protrusions depend on localised expression of Pyr, but not Ths, indicating that Pyr in the dorsal ectoderm might provide directional information (Klingseisen et al., 2009). The overall dynamics of cell movement during mesoderm spreading in *Drosophila* have recently been analysed by live imaging (McMahon et al., 2008; Murray and Saint, 2007). Cell movements were deduced from determining the positional fate of selectively labelled groups of cells using photo-activatable GFP (Murray and Saint, 2007). These analyses suggested that cells in contact with the ectoderm move dorsally during spreading. Presumably, the more internally located cells either intercalate radially or overtake cells at the dorsal edge. A second study tracked mesoderm cell nuclei labelled with GFP (McMahon et al., 2008). The authors suggested that the mesoderm spreads by synchronous waves of cell intercalation and that a stable leading cell population migrates directionally. These studies have provided important insight into the global movement of the cell collective. However, the underlying behaviour of individual cells that is responsible for the movement cannot be deduced from these studies. To understand the basis for the cell movements it is necessary to study this behaviour directly and determine how it is

controlled by the FGF receptor and its ligands. We have therefore set up an experimental system that allows us to follow cell shape changes in live-imaging experiments. We find that mesoderm cells change their behaviour several times, and that these successive cell behaviours have differential requirements for the two FGF ligands and possibly differential downstream signalling events.

MATERIALS AND METHODS

Genetics

Fly stocks were maintained under standard conditions. The following mutant alleles and transgenes used in this study have been described previously: *mys*^{1} (Wright, 1960), *mys*^{11} (Wieschaus et al., 1984), *stg*^{7M53} (Jürgens et al., 1984), *htl*^{AB42} (Gisselbrecht et al., 1996), *dof*^{1} (Vincent et al., 1998), *twi::CD2* (Dunin-Borkowski and Brown, 1995), *UAS::Cdc42[N17]* (Luo et al., 1994), *Cdc42*^{3}, *Cdc42*^{6} (Genova et al., 2000) and *shg*^{2} (Tepass et al., 1996).

Immunohistochemistry, fixed tissue imaging and measurement

Embryos were collected, fixed and stained using standard methods (Müller, 2008). Fixation was 40 minutes in 3.7% formaldehyde/PBS following manual devitellinisation. The following primary antibodies were used: rabbit-anti-Twist (1:1000), mouse-anti-Neurotactin [Developmental Studies Hybridoma Bank (DSHB); 1:50], mouse-anti-CD2 (1:500; Serotec), rat-anti-E-cadherin (1:50; DSHB) and rabbit anti-β-galactosidase (1:5000, Cappel). Secondary antibodies were conjugated to Alexa488, Alexa647 (Molecular Probes) or Cy3 (Jackson), or enzyme conjugated. Images were collected using a Leica SP2 laser scanning confocal microscope and an Olympus BX61 wide-field microscope. Homozygous recessive mutants were recognised by the absence of transgenic β-galactosidase on balancer chromosomes. Histological cross-sections were prepared as described elsewhere (Klingseisen et al., 2009). For staging, the extent of mesoderm spreading in wild type relative to the extent of germ band elongation was used. The distance from the posterior of the embryo to the posterior end of the mesoderm was measured and divided by the total embryo length. Embryos giving values of 44-53% of embryo length were considered to be in the tube-flattening phase, whereas embryos giving values from 56-59% were considered to be in the dorsal migration phase. For determination of protrusion numbers (Figs 6, 7), all protrusions were measured in a defined length of the anterior part of the germ band excluding the area where the germ band begins to curve dorsally. Positions of the tip of each protrusion and the centre of the nearest mesoderm nucleus were determined using Volocity (Improvision), with reference to images sectioned in three different planes (XY, XZ, YZ) to incorporate three-dimensional information. The distance between these positions was calculated and protrusions less than 5 μm in length were excluded. Protrusion numbers are normalised per 200 μm distance along the anteroposterior axis of the embryo.

For measurement of relative intensities of E-cadherin staining, sections were selected including areas of ectoderm and mesoderm tissue (determined by twi::CD2 staining). After measuring and subtracting the mean background staining intensity, regions of interest were drawn covering the tissues to be measured. Pixels representing the cell surfaces were selected by thresholding and mean intensities measured. Paired *t*-tests were employed to compare data from the different tissues within the same measured embryos. All measurements were carried out using ImageJ (NIH).

Molecular biology

The *twi::GFP-actin5C* was generated by cloning 3 kb genomic DNA upstream of the transcriptional start site of the *twist* gene using PCR. The EGFP-actin5C fusion was generated using pEGFP (Clontech). Both fragments were cloned into pCaSpeR 4 and transgenic lines were generated using standard protocols.

Two-photon time-lapse imaging

Embryos expressing *twi::GFP-actin5C* were prepared for imaging by a method published elsewhere (Davis, 2000). Embryos were collected, aged to stage 5, manually dechorionated, washed and oriented on agarose. They were stuck onto a cover slip coated with heptane glue, dried briefly over silica gel and covered with halocarbon 700 oil (Sigma). Images were collected using a 40× 1.3 NA oil immersion objective on an inverted Nikon Eclipse TE2000-U microscope attached to a Biorad Radiance 2100 multiphoton scanning system. A chameleon Titanium Sapphire femto-second laser (Coherent) was tuned to 895 nm to excite GFP. Signal was collected using a non-descanned light path with no emission filter to maximise collection of emitted light. The scan head was rotated so that the vertical (*y*) dimension of the captured images represents the anteroposterior axis of the embryo. In some experiments, the stage was moved along this dimension to maintain the same field of view as cells move posteriorly during germ band elongation. Scanning was unidirectional at a speed of 166 lines per second with no averaging. Laser power was adjusted to give an adequate signal-to-noise ratio while allowing normal spreading and cell division behaviour. Embryos that have been imaged under our conditions survive to hatch as viable larvae.

Image processing and visualisation

In 4D datasets, individual nuclei were tracked manually in order to follow cell movements for both the generation of movies and measurements of migration rates. Before tracking, the image stacks were processed in ImageJ (NIH) using a macro that creates stacks from projections of the original data along any of the original image axes. Using projected data in this way improves the signal-to-background ratio and allows more structures from large cells to be included (e.g. the nucleus and a cellular protrusion). At each time point, the position of the centre of each nucleus was determined manually with reference to projected data in the original (*xy*) orientation and also the two re-sliced orientations *xz* and *xy*, approximately representing transverse and saggital sections, respectively. Projections used for tracking and represented in the movies and figures were made by averaging four original image slices. Nuclear positions were recorded using the MtrackJ plug-in for ImageJ (Erik Meijering). Three-dimensional rendered images were created using Volocity (Improvision). For 3D reconstructions of two-photon data from live embryos, the autofluorescence signal from the vitelline membrane was removed by creating a binary image mask from the original data based on a defined threshold value. Masks were edited to remove any pixels representing signal internal to the embryo then dilated, to ensure that the entire signal from the membrane was covered. Masks were then blurred using a Gaussian filter and subtracted from the original image data before importing into Volocity and rendering.

RESULTS

Imaging of dynamic cell shape changes during mesoderm spreading

The mesoderm primordium invaginates by the ventral furrow forming an epithelial tube within the interior of the embryo. Reminiscent of a classic EMT, the entire tube then loses its epithelial structure and the cells adopt a mesenchymal morphology. However, unlike classic EMT, the mesoderm cells maintain an intimate contact with each other while they spread out to form a transient monolayer (Fig. 1A,B). The dynamic cell shape changes that occur during these tissue rearrangements have not been determined because of the lack of suitable imaging methods.

To monitor the dynamics of mesoderm cell morphology we used two-photon microscopy to image expression of a *GFP-Actin5C* fusion gene driven by the mesoderm-specific *twist* promoter. We are able to visualise the most superficial mesoderm cells, as well as a short distance into the cell layer lying beneath the superficial layer. GFP-Actin is abundant in cellular protrusions, allowing cell shape dynamics to be observed. Nuclei appear as dark areas, which can be used to track individual cells. To visualise different stages of the spreading movements, we adopt different protocols, varying the direction from which images are captured as well as the zoom and depth of imaging (see Fig. S1 in the supplementary material). We observe mitoses in time-lapse experiments when the reporter protein

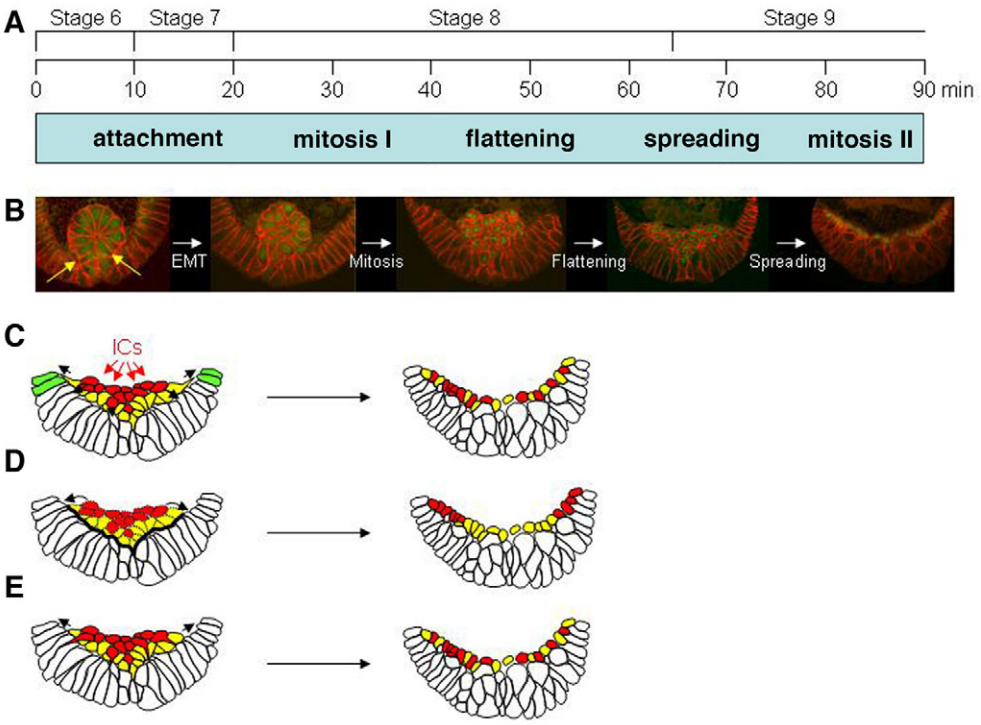

Fig. 1. Overview of mesoderm layer formation. (**A**) Approximate timeline of mesoderm behaviour during gastrulation (at 21°C). (**B**) Cross-sections of fixed embryos showing the mesoderm during dispersion (anti-Twist, green; cell surfaces, anti-Neurotactin, red). During mesoderm invagination, basal tube cells (yellow arrows) contact the ectoderm. (C-E) Models for mesoderm layer formation. (**C**) Directional migration model. Mesoderm cells that are in contact with the ectoderm surface (yellow) migrate dorsally in response to a positional cue (green). This dorsal migration creates space for inner cells (ICs, red) to intercalate radially. (**D**) Differential adhesion model. As a result of changes induced by EMT, mesoderm cells become motile and form stronger adhesions with the ectoderm than with each other. (**E**) Active intercalation model. Inner cells move actively to reach the ectoderm surface between mesoderm cells already in contact with the ectoderm. These movements displace edge cells dorsally (black arrows).

enters the nucleus upon breakdown of the nuclear envelope. Mesoderm cells divide in three waves of nearly synchronous mitoses during gastrulation, the first occurring shortly after invagination and the second at approximately the time when a cell monolayer is established, at stage 9 of embryonic development (Fig. 1A). The third division occurs later in stage 10 and coincides with segmentation of the mesoderm and its adopting a multilayered structure (Campos-Ortega and Hartenstein, 1997). We record images between the first two mitoses, allowing observation of successive changes of cell behaviour that contribute to monolayer formation.

Radial cellular protrusions during mesoderm flattening

Following invagination and EMT, mesoderm cells divide and the tissue flattens rapidly against the basal ectoderm surface. The first cellular activity of mesoderm flattening is the formation of contacts of the basal side of the mesoderm tube with the ectoderm (Fig. 1B) (Schumacher et al., 2004). It is not known whether flattening is a passive process caused by differential adhesion or whether mesoderm cells actively move towards the ectoderm.

Mesoderm-ectoderm (ME) attachment is associated with actin-rich protrusions from the mesoderm cells directed towards the ectoderm (Fig. 2). The initial region of ME contacts at the base of the tube expands during and after the period when the cells undergo EMT and divide (Fig. 1A,B). The more lateral mesoderm cells attach progressively to the ectoderm and protrude radially in between adjacent ectoderm cells. The flattening movement can thus be described as a ‘zippering-up’ of the mesoderm cell aggregate onto the ectoderm (Fig. 2A,B; see Movies 4, 5 in the supplementary material). Mesoderm cell protrusions intercalate between the basolateral surfaces of the ectoderm and are visible as concentrations of GFP-Actin at the interface between the germ layers (Fig. 2A; see Movie 4 in the supplementary material). These cell shape changes are associated with cell movement. Cells located at the dorsolateral edges of the mesoderm (dorsal edge cells, DECs) move radially outwards from central towards more peripheral positions (Fig. 2B; see Movie 5 in the supplementary material). Large radial protrusions (19.0 μm±2.7 (s.d.; n=7 from three embryos) are seen in these cells and also at more ventral positions (Fig. 2C; see Movie 6 in the supplementary material). We conclude that the major initial movement of mesoderm cells is radial and is an active process, probably driven by actin-rich protrusions extending from the mesoderm cells.

Mesoderm-ectoderm attachment is associated with local E-cadherin accumulation

The discovery that the *Drosophila* mesoderm forms an intimate connection with the ectoderm following internalisation is unexpected. During gastrulation in vertebrates, cell signalling events trigger repulsion between mesoderm and ectoderm, and an extracellular matrix is established at the germ layer interface (Chuai and Weijer, 2009b; Winklbauer et al., 2001).

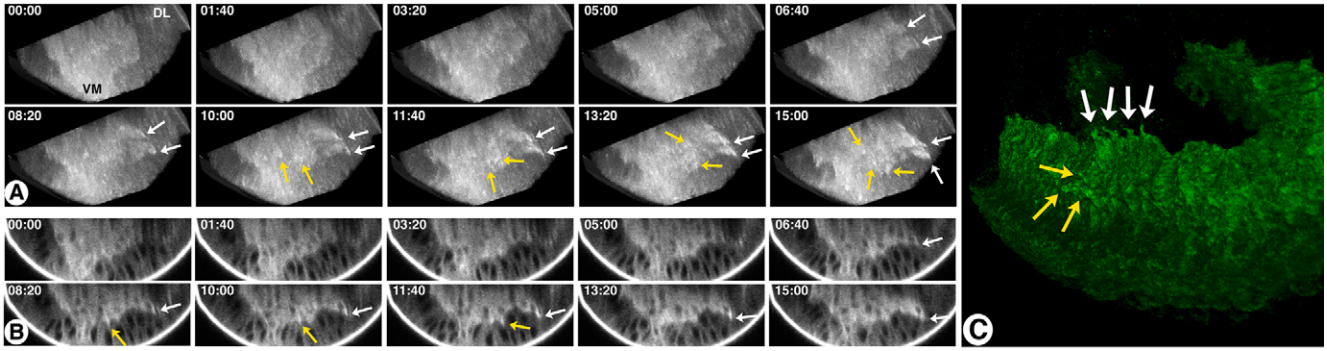

Fig. 2. Protrusion formation during mesoderm flattening. (**A**,**B**) Two-photon time-lapse sequence of mesoderm cells expressing GFP-Actin in the period following EMT (ventral imaging protocol; see Fig. S1 in the supplementary material). VM, ventral midline; DL, dorsolateral ectoderm. (A) Intensity-rendered 3D reconstructions (see Movie 4 in the supplementary material); (B) transverse sections (see Movie 5 in the supplementary material). Cells at the dorsal edge (DECs) protrude radially (white arrows) and move towards the ectoderm (yellow arrows indicate ventral cells protruding into the ectoderm). (**C**) DEC (white arrows) and more ventral cell (yellow arrows) protrusions visualised in a wild-type *twi::CD2*-expressing embryo fixed during mesoderm flattening (3D reconstructed image shown rotating in Movie 6 in the supplementary material). Embryo in C is shown in ventrolateral view, anterior towards the left.

It has been proposed that integrin-mediated contacts are responsible for high-affinity ME interactions in *Drosophila* (McMahon et al., 2010; Murray and Saint, 2007). β1-myospheroid (*mys*) integrin complexes become concentrated at the ME interface in the late stages of spreading (Leptin et al., 1989; McMahon et al., 2010). It has recently been reported that embryos maternally and zygotically (M/Z) mutant for the mys^{1} allele exhibit defects in monolayer formation (McMahon et al., 2010). mys^{1} M/Z mutant embryos show abnormal monolayer formation, reduced dorsal mesoderm differentiation and fewer DEC protrusions (Fig. 3B,D,E). The molecular lesion in mys^{1} is described as a chromosomal deletion, but the extent of this chromosomal rearrangement has not been determined (Bunch and Brower, 1992). As the molecular lesion of the mys^{1} allele is not unambiguous, we repeated these experiments with the protein null allele mys^{11} (Bunch and Brower, 1992; Jannuzi et al., 2002; Leptin et al., 1989). mys^{11} M/Z mutants exhibit normal mesoderm migratory morphology, normal monolayer formation and dorsal mesoderm specification (Fig. 3A,C,E). These data indicate that the mys^{1} allele is associated with other mutations on the chromosome that alone or in combination produce mesoderm-spreading defects. We conclude that β1-integrin function is not required for mesoderm spreading.

As integrin-mediated adhesion is dispensable for ME attachment we reasoned that direct cell-cell contacts may be responsible. It has been suggested that ME separation represents a classic example of tissue separation via differential expression of cadherins (Oda and Tsukita, 1999). Consistent with this model is the observation that E-cadherin transcription is repressed by Snail and N-cadherin transcription is upregulated by Twist (Oda and Tsukita, 1999). However, N-cadherin protein accumulates in the mesoderm only at later stages during monolayer formation (Oda and Tsukita, 1999). We find that throughout mesoderm spreading, the maternally provided E-cadherin remains present in mesoderm cells (Fig. 3F-I). Measurements of the fluorescence intensity of E-cadherin immunolabeling revealed that the intensity at ectoderm/ectoderm cell contacts was not significantly different from that of mesoderm/mesoderm contacts [P=0.39 (n=5); paired t-test]. By contrast, the level of E-cadherin at the mesoderm/ectoderm interface is elevated, in comparison with cell-cell contacts within either the mesoderm [P=0.00088 (n=5); paired t-test] or the basolateral domain of ectoderm cells [P=0.00067 (n=5); paired t-test] (Fig. 3F,G). E-cadherin is also accumulated at sites where mesodermal protrusions penetrate between ectoderm cells (Fig. 3H,I; see Movie 7 in the supplementary material). The high E-cadherin staining intensity at these sites is not simply a consequence of the closely apposed membranes of the protrusion, as the raised level of E-cadherin is also seen at protrusions where the membranes can be distinguished from each other (Fig. 3H). A similar accumulation it is not seen for other membrane proteins, such as neurotactin (not shown). Consistent with a role of E-cadherin in mesoderm layer formation, embryos mutant for the E-cadherin loss-of-function allele shg^{2} (*shotgun*) exhibit various defects in mesoderm morphogenesis and dorsal mesoderm differentiation (see Fig. S2 in the supplementary material). These observations indicate that E-cadherin is recruited to ectoderm/mesoderm contacts and suggest that the intercalation of mesoderm cells into the ectoderm involves direct cell contacts mediated by E-cadherin.

Repolarisation and migration of dorsal edge cells

In the first phase of mesoderm spreading, EMT and mesoderm flattening increase the number of cells in contact with the ectoderm; however, not all mesoderm cells have made contact with the ectoderm at the end of this phase. Various mechanisms have been proposed to account for the mesoderm layer formation (Fig. 1C-E) (Kadam et al., 2009; Klingseisen et al., 2009; McMahon et al., 2008; Murray and Saint, 2007; Wilson et al., 2005; Winklbauer and Müller, 2011). We analysed the behaviour of DECs of the mesoderm as we have shown before that protrusions at the dorsal edge are sensitive to the availability of FGF8-like ligands.

Live observations of DECs reveal that their movement follows a stereotypic biphasic pattern. During flattening, DECs initially protrude radially with little net dorsal movement. During a 15-20 minute period after the first mitotic wave, all DECs (n=12; three embryos) extend protrusions in a radial direction between ectoderm cells (Fig. 2A-C; Fig. 4A). As the cells move radially outwards, these radial protrusions become shorter and eventually disappear (Fig. 4A; see Movie 8 in the supplementary material). DECs then

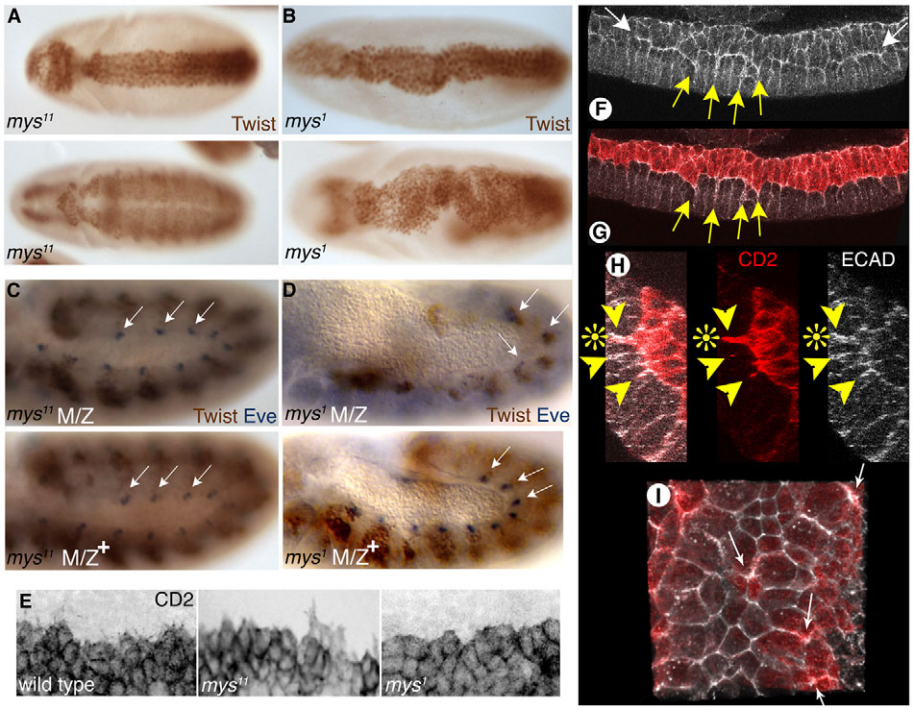

Fig. 3. Contribution of integrin and E-cadherin to ME contact. (A,B) Ventral views (anterior leftwards) of fixed embryos during mesoderm flattening (top panels) and post-spreading (lower panels) (anti-Twist, brown). (**A**) *mys*^{11} maternal-zygotic mutants show normal flattening and monolayer formation. (**B**) *mys*^{1} matermal zygotic mutants exhibit defects in flattening and monolayer formation. (**C**,**D**) Lateral views of extended germ band embryos [stage 11 (C) or stage 12 (D)] stained for Twist (brown) and the dorsal mesoderm marker Even Skipped (Eve) (dark purple); the upper panels show embryos that are maternally and zygotically mutant (M/Z), whereas the lower panels show maternal mutants that express a wild-type *mys* allele in the zygote from the paternal chromosome (M/Z^{+}). (C) Eve-positive dorsal mesoderm precursors are specified normally in *mys*^{11} mutants (white arrows). (D) In *mys*^{1} M/Z mutants, but not M/Z^{+} mutants, dorsal mesoderm differentiation is impaired (white arrows). (**E**) DEC morphology shown by CD2 staining of wild-type, *mys*^{11} MZ and *mys*^{1} MZ mutant embryos. Ventrolateral aspect focussed on the dorsal edge of the mesoderm (anterior leftwards). (**F**,**G**) Confocal section through the ventrolateral germ band (lateral view; anterior leftwards; red, CD2 expressed in the mesoderm; white, E-cadherin). In wild-type embryos, E-cadherin accumulates at radial mesoderm protrusions (yellow arrows) and the ME interface (white arrows in F). (**H**) Virtual cross-section through ventral area of ME contact showing radial protrusions associated with high local concentrations of E-cadherin (yellow arrowheads). Asterisks mark a protrusion that is delineated by E-cadherin staining. (**I**) Volume-rendered 3D-reconstruction viewed through the lateral ectoderm (white arrows indicate positions of radial protrusions; see Movie 7 in the supplementary material).

repolarise and switch from radial movement to a persistent dorsal migration during the following 30-40 minutes. Thereafter, they undergo the second wave of mitotic divisions. Tracking nuclear positions of DECs over time confirms a biphasic migration of DECs, first in a radial direction and then in a dorsal direction (Fig. 4D).

Repolarisation is associated with remodelling of the protrusive activity of DECs. Half of the DECs we imaged (6/13; three embryos) formed new protrusions, oriented in the direction of spreading, as they began their dorsal migration (Fig. 4A,B; see Movie 8 in the supplementary material). Imaging DECs at higher resolution reveals a polarised morphology that is indicative of directionally migrating cells (Fig. 4B; see Movie 9A in the supplementary material). DECs extend and polarise along the direction of migration and form lamellipodia and filopodia. The distance from the front edge of the nucleus to the tip of the lamellipodium can extend up to 17 μm, whereas the cell body diameter (distance between the centres of adjacent nuclei) is 7.1 μm (±1.1; n=6). Filopodia are believed to contribute a sensory function during migration by sampling the environment for directional cues (Millard and Martin, 2008). We observe dynamic filopodia extending from the leading edge cells (Fig. 4C; see Movie 9B in the supplementary material). The polarised morphology of DECs and the presence of filopodia at their leading edge suggest that these cells migrate directionally towards a dorsal attractant.

Although DECs retract their radial protrusions as they repolarise and migrate dorsally, the more ventrally located cells maintain radial protrusive activity throughout the period of dorsal spreading. Large, dynamic protrusions extend deep into the ectoderm, disappearing only as cells round up at the next wave of mitosis as the monolayer forms (Fig. 4E; see Movie 10 in the supplementary material). These results demonstrate continuous intercalation behaviour of mesoderm cells and a dynamic interaction with the basal-lateral domain of the ectoderm throughout the spreading process. The dorsal movement of DECs also reduces space constraints for inner cells and might thereby promote their movement to the ectoderm surface (Fig. 1C). Indeed, tracking of mesoderm nuclei in live embryos has suggested that the majority of inner mesoderm cells reach the surface by this route (McMahon et al., 2008), and we observe this cell behaviour directly in our time-lapse experiments (see Movie 11 in the supplementary material). These results demonstrate that, after flattening, mesoderm cells maximise their contact to the ectoderm surface by two major movements: directional migration of dorsal edge cells and radial intercalation movements of inner cells.

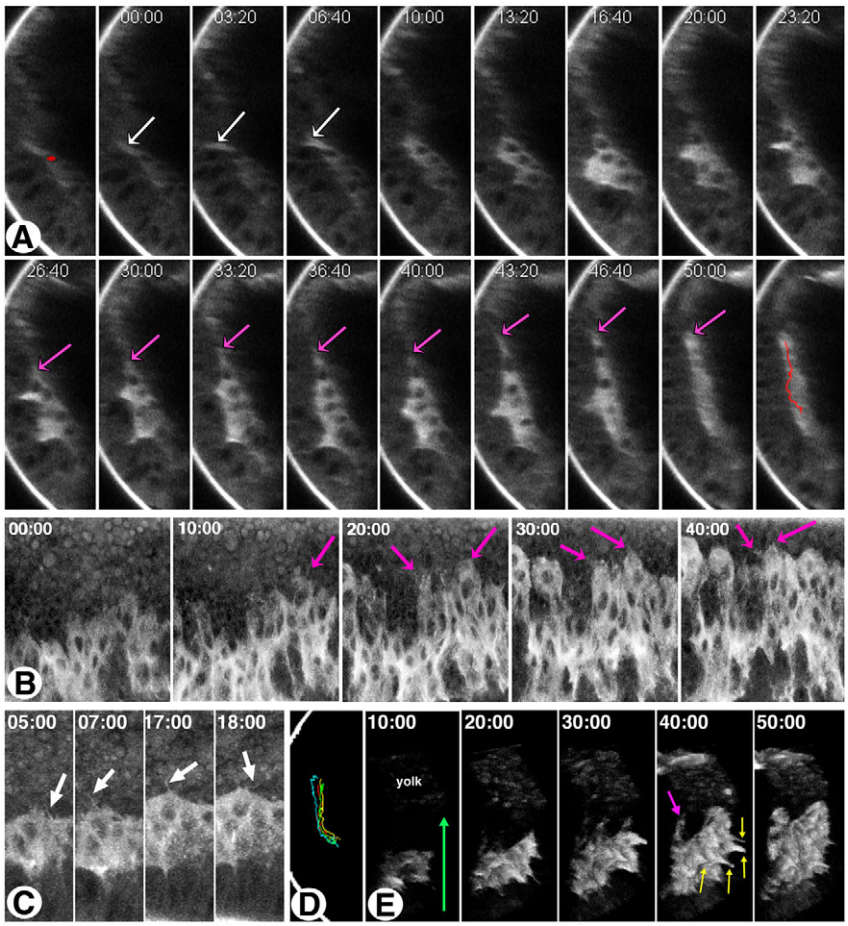

Fig. 4. Biphasic movement of DECs and dorsal migration. (**A**) Two-photon time-lapse sequence of mesoderm cells expressing GFP-actin visualised as transverse sections (ventral-lateral protocol, see Fig. S1 in the supplementary material; see Movie 8 in the supplementary material). The ventral midline is towards the right, but is not present in the image. Radial protrusions are marked with white arrows. DECs repolarise and extend lamellipodia dorsally (magenta arrows). Tracking of individual DEC nuclei reveals biphasic movement (track of cell marked with red dot in the first frame is shown in the last frame of A; further tracks in D). (**B**) Dynamics of DEC dorsal migration (magenta arrows indicate lamellipodia). Two-photon time-lapse sequence visualised as maximum projections from ventrolateral view (dorsal edge imaging protocol, see Fig. S1 in the supplementary material; see Movie 9A in the supplementary material). (**C**) Dynamic filopodia (white arrows) at leading edge of dorsal cells. Maximum projected image stacks captured at 20-second intervals (dorsal edge imaging protocol; see Movie 9B in the supplementary material). (**D**) Superimposed tracks showing biphasic movements of four individual DEC nuclei during spreading. (**E**) Three-dimensional reconstructed images indicate dynamic radial mesoderm protrusions (yellow arrows) extending into the ectoderm (dorsally directed lamellipodia are marked with magenta arrows; see Movie 10 in the supplementary material). The green arrow in the first frame indicates the dorsal direction.

Redistribution of E-cadherin during EMT requires FGF signalling

Mesoderm layer formation requires FGF signalling, and we have shown previously that ME attachment prior to EMT depends on Htl (Schumacher et al., 2004), Having identified several successive cellular behaviours during mesoderm layer formation, we wished to determine how these behaviours are affected by FGF signalling.

As FGF is known to be important for EMT in vertebrates, we first analysed the role of FGF in the transition from the epithelial invaginated mesoderm to a mesenchymal state. During formation of the blastoderm epithelium, E-cadherin accumulates at sub-apical adherens junctions. In the mesoderm, the early adherens junctions are disassembled and re-established at the extreme apical site (Kölsch et al., 2007), where they are maintained until after formation of the mesoderm tube (Fig. 5). As EMT occurs, E-cadherin loses its apical concentration and redistributes over the mesoderm cell surfaces in a non-polarised fashion (Fig. 5). At the same time, cells begin to divide, but the loss of cell contact is not exclusively due to cells rounding up in mitosis, as it is also seen in embryos mutant for *string* (*stg*), in which post-blastoderm mitoses are blocked (Fig. 5A,B) (Leptin and Grunewald, 1990). Thus, EMT can occur independently of mitotic divisions, implying that other processes remodel cell polarity and epithelial junctions.

One possibility is that FGF signalling contributes to EMT. It is not possible to test this simply by disrupting FGF signalling, as mitosis still occurs and cells therefore lose their contacts. To test for a possible role for FGF signalling in EMT it is necessary to interfere with FGF signalling in a situation where mitosis does not occur. We thus created embryos that were simultaneously mutant for *stg* and the FGF receptor Htl or the FGF signal transducer Dof. In *htl stg* or *dof stg* double mutants, mesoderm cells maintain their epithelial state and show persistent polarised E-cadherin distribution and maintenance of junctions after invagination (Fig. 5A,B; data not shown). The block of EMT is transient, but results in strongly delayed spreading and monolayer formation (Wilson et al., 2005) (see Fig. S3 in the supplementary material). This result implies a role for FGF signalling in the remodelling of polarised E-cadherin adhesion during the onset of EMT in the mesoderm.

FGF8-like ligands control protrusive activity during mesoderm-ectoderm attachment

ME attachment and mesoderm flattening are impaired in the absence of FGF signalling (Schumacher et al., 2004; Wilson et al., 2005). Embryos lacking Htl develop fewer and shorter mesodermal protrusions (see Fig. S3 and Movie 12 in the supplementary material), and there is little radial cell movement (data not shown). The absence of early pre-EMT protrusions at the base of the tube in *htl* and *dof* mutant embryos suggests functions of FGF signalling other than the control of EMT (Wilson et al., 2005). To determine the role of the Htl ligands Pyr and Ths for protrusive activity of mesoderm cells after EMT, we studied mutants lacking either one of the ligands. The number of protrusions was determined in tightly staged embryos, fixed during mesoderm flattening or during dorsal migration of DECs (Fig. 6A-D).

Although embryos lacking *ths* function have the normal number of protrusions during flattening, *pyr* mutant embryos show a reduction in protrusions, both in the dorsal and in ventrolateral cells

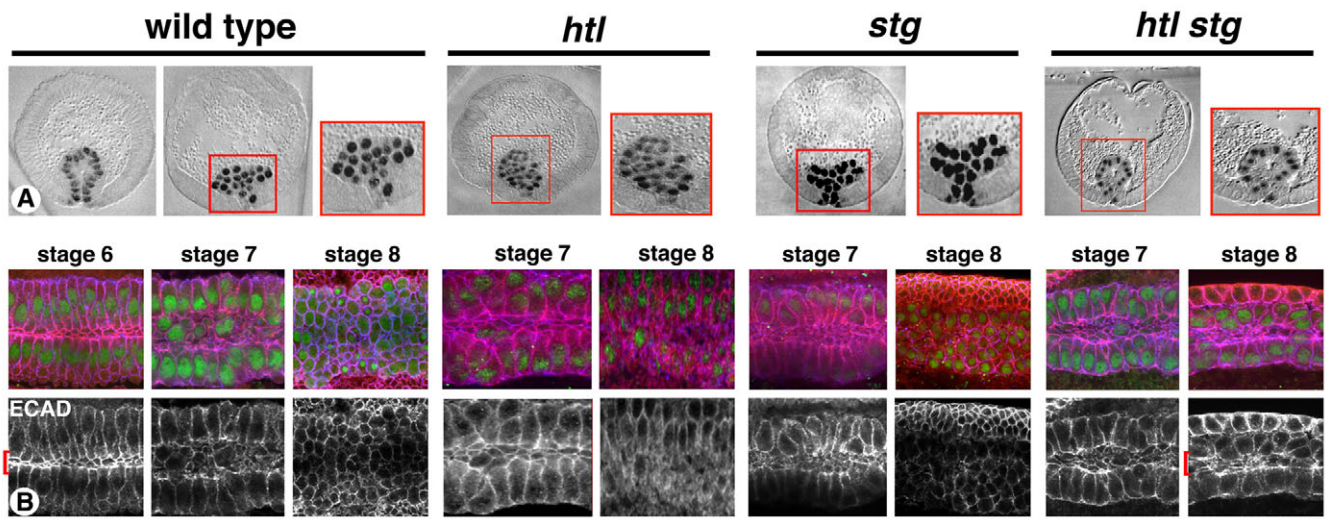

Fig. 5. *htl* is required for loss of epithelial polarity during EMT. (**A**) Transverse cross-sections (dorsal upwards; ventral at the bottom) of wild-type, *htl*, *stg* and *htl stg* homozygous embryos at early stage 8; the embryo on the very left is at stage 7 (anti Twi in black). Mesoderm cells lose their tube-like epithelial organisation in wild-type embryos and *htl* or *stg* homozygotes. In *htl stg* double mutants, cells retain their tube-like organisation into stage 8. (**B**) Confocal optical sections through embryos (anterior leftwards) immunolabelled for E-cadherin (red), Neurotactin (blue) and Twist (green). E-cadherin signal is also shown in grayscale in lower panels (ECAD). Genotypes and stages are indicated. Representative confocal sections are taken through the central region of the mesoderm. During stage 7 and 8, E-cadherin becomes redistributed in the mesoderm cells (apical accumulation of E-cadherin marked with red bracket in left panel). In *htl*,*stg* homozygotes, polarised E-cadherin is maintained in stage 8 (red bracket in right panel).

(Fig. 6C). The phenotype is not as severe as in embryos lacking Htl, which suggests redundancy between Pyr and Ths functions. We conclude that FGF signalling has independent functions in the transition to a mesenchymal state and the formation of protrusions associated with the orderly flattening of the mesoderm onto the ectoderm surface.

Pyr is required for normal dorsal migration rates of DECs

DEC morphology during later mesoderm spreading suggested that after flattening, cells migrate dorsally in response to directional cues. An obvious candidate for a dorsal attractant is Pyr. Its expression becomes largely restricted to a dorsal domain of the ectoderm when dorsal spreading occurs (Gryzik and Müller, 2004; Stathopoulos et al., 2004) and it is necessary for the formation of DEC protrusions (Fig. 6B,D). We asked whether reduced numbers of dorsal protrusions in pyr^{18} mutants are reflected in a difference in the migratory behaviour of DECs. Wild-type DECs move dorsally with a mean rate of 52.7±3.0 μm/h (n=13; three embryos). This is comparable with the migration speeds of other *Drosophila* cells that move in collectives, e.g. ovarian border cells [21-60 μm/h (Bianco et al., 2007; Prasad and Montell, 2007; Tekotte et al., 2007)] and male-specific SGPs [(12.3 μm/h) (Clark et al., 2006)]. The mean migration rates of DECs were significantly lower in pyr^{18} homozygous mutants (21.4±4.1 μm/h; n=9; two embryos), showing that Pyr is necessary for the directional dorsal migration of DECs (Fig. 6F; see Movie 13 in the supplementary material). These experiments demonstrate that Pyr represents a dorsal cue providing a significant influence on the direction and the speed of dorsal mesoderm cells.

Throughout the dorsal migration phase, the ventral mesoderm cells exhibit a dynamic radial protrusive activity (Fig. 4E). We found that Ths, and to a lesser extent also Pyr, are required for the normal number of these radial protrusions during dorsal migration (Fig. 6D). However, in neither of the single mutants are radial protrusions completely abolished, suggesting that Ths and Pyr contribute together to this activity.

Cdc42 is required for the formation of radial protrusions and for the accumulation of E-cadherin at the mesoderm-ectoderm interface

To explore the functional importance of the radial protrusions for mesoderm spreading, we sought to identify a way to interfere selectively with their formation. As filopodial protrusions often depend on the activity of the small Rho GTPase Cdc42, we examined protrusion formation in embryos in which we had interfered with Cdc42 function by expressing a dominant-negative construct, Cdc42[N17], in the mesoderm. Formation of radial protrusions was strongly compromised upon expression of Cdc42[N17], whereas the number of dorsal protrusions did not change significantly (Fig. 7A). These data provide evidence that dorsal and radial protrusions are controlled by distinct molecular pathways. Consistent with a role for Cdc42 in mesoderm morphogenesis, embryos in which Cdc42 activity is reduced exhibit defects in mesoderm layer formation and dorsal mesoderm differentiation (Fig. 7B). To investigate whether the reduction of radial protrusions in mesoderm cells expressing Cdc42[N17] correlates with defects in redistribution of E-cadherin at the germ layer interface, we examined E-cadherin localisation in those embryos (Fig. 7C). In contrast to our findings in the wild type, where E-cadherin is enriched at the ectoderm/mesoderm interface, in embryos expressing Cdc42[N17] we found no difference in E-cadherin immunoreactivity at the mesoderm/ectoderm interface compared with either mesoderm/mesoderm [P>0.1 (n=3); paired t-test] or ectoderm/ectoderm [P>0.05 (n=3); paired t-test] contacts. These data implicate Cdc42 function in the recruitment of E-cadherin to the mesoderm-ectoderm interface.

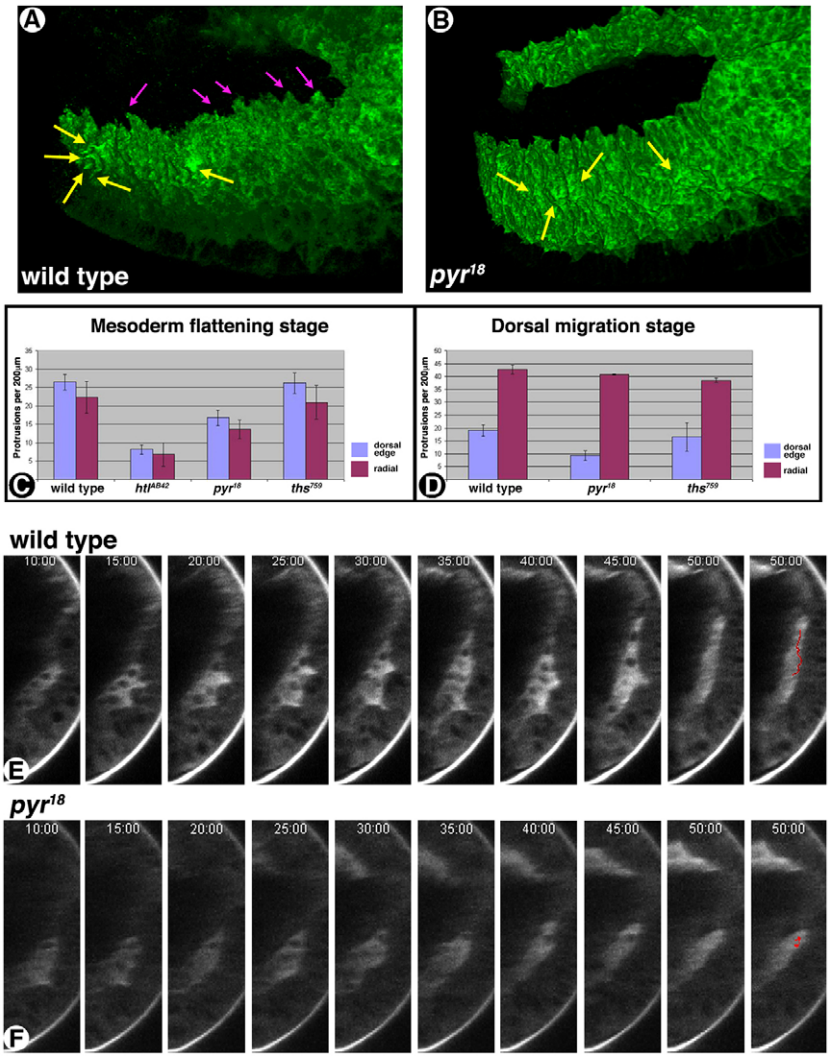

Fig. 6. FGF8-like ligands in protrusion formation and dorsal migration. (**A**,**B**) Pyr is required for a normal number of dorsal edge protrusions during dorsal spreading. Volume-rendered 3D reconstructions of wild type (A) and *pyr*^{18} homozygotes (B) expressing *twi:CD2* (green; ventrolateral views, anterior towards the left). Dorsal edge (magenta arrows) and radial (yellow arrows) mesodermal protrusions are indicated. (**C**) Quantification of dorsal edge (blue) and radial (purple) protrusions in embryos of the indicated genotypes (CD2 staining of *htl* and *htl,stg* homozygotes are shown in Fig. S3 in the supplementary material) (see also Movie 12 in the supplementary material). Data are shown for the flattening period (**C**) and for the dorsal migration phase (**D**) (mean±s.e.m.). (**E**,**F**) Reconstructed transverse sections of two-photon time lapse sequences of wild-type (E) and homozygous *pyr*^{18} (F) mutant embryos expressing *twi::GFP-Actin* (ventral-lateral protocol; see Fig. S1 in the supplementary material). Images represent 40 minutes prior to entry into the second mitosis (see Movie 13 in the supplementary material). The orientation of the embryos is ventral downwards and dorsal pointing upwards.

DISCUSSION

In vertebrate gastrulation, FGF signalling has been implicated in EMT, ingression and guidance of mesoderm cells away from the primitive streak (Chuai and Weijer, 2009a; Thiery et al., 2009). We have identified successive cellular activities and behaviours during *Drosophila* mesoderm layer formation. Our results now allow the integration of the previously described dynamic observations of tissue movements with the shape changes of individual mesoderm cells. We find that the two FGF ligands, Pyr and Ths, have multiple, partially overlapping functions in directing this morphogenetic behaviour.

FGF signalling drives protrusive activity during mesoderm flattening

The rapid flattening of the mesoderm onto the ectoderm surface has been attributed to decreased adhesion between mesoderm cells as a result of the mitotic division that follows internalisation (Murray and Saint, 2007). An alternative view proposed that the mesoderm actively contact the ectoderm involving mesoderm cell protrusions (Schumacher et al., 2004). We now find that the mesoderm extends actin-rich protrusions towards the ectoderm as the tissue flattens. The formation of these protrusions depends on FGF signalling, which suggests a role for the FGF pathway in controlling the dynamics of the actin cytoskeleton.

Mesoderm flattening occurs by a zippering motion, with progressive attachments that commence in the most ventral region and propagate to more dorsolateral positions (Fig. 8A). We propose that the region in which protrusions are formed expands dorsally, because flattening of ventral parts of the mesoderm exposes more dorsally located cells to the influence of FGF expressed by the neuroectoderm. This propagation model of mesoderm flattening helps to explain on a cellular level how cells from defined initial positions follow apparently stereotypical paths (McMahon et al., 2008; Murray and Saint, 2007). Such a mechanism would provide for an orderly association of the germ layers, ensuring that mesoderm cells are symmetrically distributed about the ventral midline (Fig. 8A).

Mesoderm-ectoderm adhesion

It has been proposed that mesoderm spreading may be driven by differential adhesion (Murray and Saint, 2007; Wilson et al., 2005). A propensity for the mesoderm to maximise contact with the ectoderm would follow from mesoderm cells that exhibit a higher affinity for the ectoderm than for each other. Consistent with earlier studies (Oda et al., 1998), we find that although E-cadherin transcription is repressed by Snail in the mesoderm, maternal E-cadherin protein levels do not rapidly decrease upon EMT. During EMT, E-cadherin distributes over the whole cell surface of the

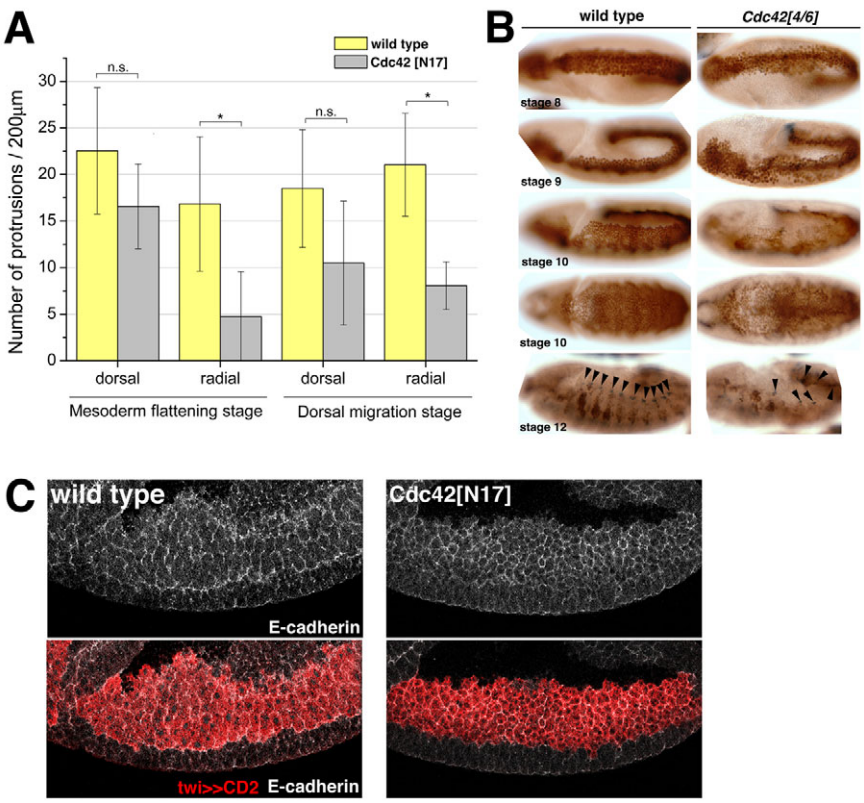

Fig. 7. A role for Cdc42 at the mesoderm/ectoderm interface. (**A**) Comparison of dorsal and radial protrusions (from *twi::CD2* stainings) in wild-type embryos (yellow bars) and embryos expressing *UAS::Cdc[N17]* driven by *twi::Gal4*. The asterisks indicate statistically significant differences in the number of radial protrusions [$P<0.05$ ($n=5$); two-sample *t*-test]. There is no difference in the number of dorsal protrusions [$P>0.05$ ($n=5$); two-sample *t*-test]. Data are mean±s.d. (**B**) Wild-type and Cdc42 mutant embryos (obtained from $Cdc42^{4}/Cdc42^{6}$ trans-heterozygous females) were stained for Twi (stages 8-10) and for Eve (stage 12). Note irregular distribution of mesoderm nuclei in Cdc42 mutants compared with wild type, indicating defects in mesoderm spreading. Arrowheads in stage 12 embryos indicate position of segmental Eve-positive dorsal mesoderm cells; note the strong reduction in the number of Eve-positive hemi-segments. (**C**) E-cadherin immunostaining of embryos (stage 9) expressing *UAS::Cdc[N17]* driven by *twi::Gal4* compared with wild type. E-cadherin accumulates at the ectoderm-mesoderm interface (mesoderm is marked in red with CD2), which is absent in embryos expressing dominant-negative Cdc42.

mesoderm cells. As contact with the ectoderm is made, E-cadherin accumulates at the germ layer interface, including the sites where mesodermal protrusions penetrate the ectodermal layer. E-cadherin mutants exhibit mild defects in dorsal mesoderm morphogenesis, but we do not yet understand the function of E-cadherin in differential adhesion or in promoting mesoderm-ectoderm attachment and spreading. To address this issue, it will be necessary to establish a system for tissue-specific conditional interference with E-cadherin.

It is also possible that molecules other than E-cadherin mediate adhesion between the ectoderm and the mesoderm germ layer. Although the prime candidate for this mechanism is integrin-mediated adhesion, we find no evidence for a role of integrins in mesoderm spreading, confirming earlier studies (Bunch and Brower, 1992; Jannuzi et al., 2002; Leptin et al., 1989). We therefore favour the model that E-cadherin has a major role in establishing adhesion between the germ layers.

FGF signalling contributes to a switch in the state of E-cadherin leading to the redistribution of polarised E-cadherin during EMT in the invaginated mesoderm cells. A similar switch in E-cadherin function occurs during border cell migration in *Drosophila* oogenesis (Niewiadomska et al., 1999). Although the cytoplasmic domain of E-cadherin contains a conserved function necessary for cell migration (Pacquelet and Rorth, 2005), it is unclear how the E-cadherin in migrating cell collectives is linked to the cytoskeleton to allow it to transmit the forces required for movement. The cell contacts involved in these movements need not be stable adherens junctions, but are perhaps rather dynamic interactions. Our study identifies Cdc42 as an important determinant of both protrusion formation and E-cadherin accumulation at the ectoderm/mesoderm interface. Further studies will have to address the mechanisms by which Cdc42 is controlled and functions upstream of E-cadherin localisation.

Mesoderm layer formation results from distinct cell movements

Our study has revealed that dorsal edge cells undergo successive changes in protrusive behaviour (Fig. 8B). The biphasic movement of DECs and repolarisation of protrusive behaviour correlate in timing with the switch in *pyr* mRNA distribution to a more restricted expression in the dorsal ectoderm (Gryzik and Müller, 2004; Stathopoulos et al., 2004). We show that Pyr is indeed required for the normal migratory behaviour of cells at the dorsal edge. We propose that as DECs migrate dorsally, opportunities are created in their wake for the intercalation of inner mesoderm cells into the monolayer more ventrally (Fig. 8B).

The relevance of the radial protrusive activity for mesoderm spreading is less easy to understand. Pyr and Ths are both required for E-cadherin redistribution and radial protrusion formation during mesoderm flattening. The patterns of the paths derived by tracking all mesodermal cells have hinted at intercalation as an important mechanism of mesoderm layer formation (McMahon et al., 2008). The radial protrusive activity indicates a continuous attraction of mesoderm protrusions towards the ectoderm. We propose that a main function of FGF signalling on a cellular level is to direct protrusive activity into two overall directions: dorsal and radial. We have shown earlier that dorsal protrusions depend on the Rac pathway (van Impel et al., 2009), whereas we show here that radial protrusions are particularly sensitive to loss of Cdc42 function. These results suggest that FGF signals might be differentially transduced within the migrating collective or that radial protrusive activity uses distinct molecular pathways.

Conclusion

Based on the evidence presented here and in other studies, we propose that FGF signalling performs three key functions in controlling mesoderm cell behaviour (Fig. 8C): (1) FGF triggers

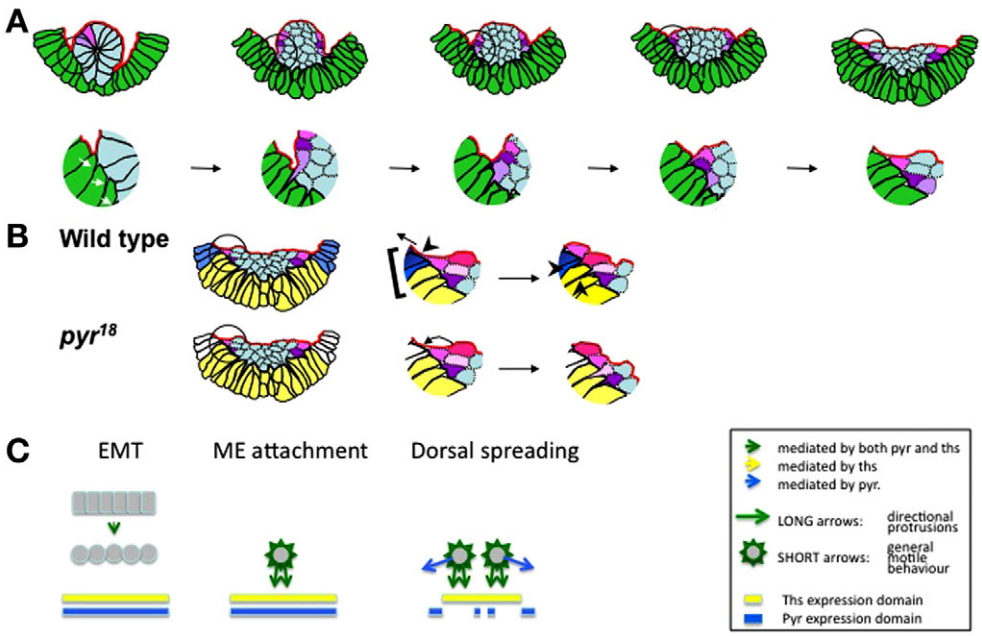

Fig. 8. Model of successive cell behaviours during mesoderm dispersion. (**A**) Progressive mesoderm flattening. During invagination, protrusions (white arrows) are formed that link ventral mesoderm cells with the underlying ectoderm (mesoderm, cyan; ectoderm co-expressing Pyr and Ths, green; yolk membrane, red). After EMT, adhesion is established through E-cadherin at the ME interface (thick black line), although adhesion between mesoderm cells may become weaker (broken lines). Cells near the base of the tube (purple) experience a gradient of FGF and form radial protrusions. They move to the ectoderm, displacing the yolk membrane and thus allow dorsal cells (magenta) to experience the FGF gradient and protrude. The mesoderm flattens by zippering through progressive protrusion formation. (**B**) The expression of Ths becomes restricted to a ventral domain (yellow), whereas Pyr is present in the dorsal neuroectoderm (blue). Local consumption or degradation of Pyr may create and renew a gradient ofligand (square bracket) leading to DEC polarisation (black arrowhead in centre image). Dorsal migration of DECs (magenta, black arrow shows movement) creates space for inner cells (light and dark pink) to intercalate to the ectoderm surface. Ths expression supports radial protrusions (black arrowheads in right image). (**C**) Cellular mechanisms driven by FGF ligands in mesoderm spreading. Pyr and Ths together contribute to EMT and establishing migratory behaviour. They combine to induce directional protrusions that promote ME attachment. Later, dorsal Pyr expression is required for dorsal migration. Ventrolateral expression of Ths contributes to radial protrusive activity together with Pyr, which is expressed in small ventral patches.

actin-dependent protrusive activity during flattening; (2) FGF induces modulation of E-cadherin distribution during EMT; (3) FGF acts as an attractant for dorsal migration. Therefore, the key cellular processes that depend on FGF are the remodelling of E-cadherin adhesions and the guidance of directional protrusive activity. Although the molecular details of the signalling pathways remain to be discovered, our data suggest that distinct small GTPase pathways, such as Cdc42 and Rac, play crucial roles in determining the specificity of the FGF signalling responses that direct cell behaviours during mesoderm layer formation.

Acknowledgements
We thank Sabine Schumacher for construction of the twi-GFP-actin5C transgenes and Sam Swift and Paul Appleton and the staff of the Centre for High resolution Imaging at the College of Life Sciences (Dundee) for support and discussions. We thank Nick Brown and the Bloomington stock centre for fly stocks, Ryan Webster for expert technical assistance and Sirin Otte for her contribution to the EMT study. We thank David Finnegan for hosting IBNC during the final stages of this work. We thank Rudi Winklbauer, Kees Weijer and members of the H.-A.J.M laboratory for discussions and critical comments on the manuscript. Flybase was used as a reference source throughout this work. This work was funded by a MRC Non-Clinical Senior Fellowship (GO0501679) and MRC project grant (GO0901020) to H.-A.J.M. and by funds from the College of Life Sciences, University of Dundee. Deposited in PMC for release after 6 months.

Competing interests statement
The authors declare no competing financial interests.

Supplementary material
Supplementary material for this article is available at
http://dev.biologists.org/lookup/suppl/doi:10.1242/dev.060277/-/DC1

References

Beiman, M., Shilo, B. Z. and Volk, T. (1996). Heartless, a Drosophila FGF receptor homolog, is essential for cell migration and establishment of several mesodermal lineages. *Genes Dev.* **10**, 2993-3002.
Bianco, A., Poukkula, M., Cliffe, A., Mathieu, J., Luque, C. M., Fulga, T. A. and Rorth, P. (2007). Two distinct modes of guidance signalling during collective migration of border cells. *Nature* **448**, 362-365.
Biname, F., Pawlak, G., Roux, P. and Hibner, U. (2010). What makes cells move: requirements and obstacles for spontaneous cell motility. *Mol. Biosyst.* **6**, 648-661.
Bunch, T. A. and Brower, D. L. (1992). Drosophila PS2 integrin mediates RGD-dependent cell-matrix interactions. *Development* **116**, 239-247.
Campos-Ortega, J. A. and Hartenstein, V. (1997). In *The Embryonic Development of Drosophila melanogaster*, pp. 9-102. Berlin, Heidelberg: Springer Verlag.
Chuai, M. and Weijer, C. J. (2009a). Regulation of cell migration during chick gastrulation. *Curr. Opin. Genet. Dev.* **19**, 343-349.
Chuai, M. and Weijer, C. J. (2009b). Who moves whom during primitive streak formation in the chick embryo. *HFSP J.* **3**, 71-76.
Ciruna, B. and Rossant, J. (2001). FGF signaling regulates mesoderm cell fate specification and morphogenetic movement at the primitive streak. *Dev. Cell* **1**, 37-49.
Clark, I. B., Boyd, J., Hamilton, G., Finnegan, D. J. and Jarman, A. P. (2006). D-six4 plays a key role in patterning cell identities deriving from the Drosophila mesoderm. *Dev. Biol.* **294**, 220-231.
Costa, M., Sweeton, D. and Wieschaus, E. (1993). Gastrulation in Drosophila: cellular mechanisms of morphogenetic movements. In *The Development of Drosophila melanogaster*, Vol. 1 (ed. M. Bate and A. Martinez Arias), pp. 425-465. Plainview, NY: Cold Spring Harbor Laboratory Press.

Davis, I. (2000). Visualising fluorescence in Drosophila: optimal detection in thick specimens. In *Protein Localisation by Flourescence Microscopy: A Practical Approach* (ed. V. Allan), pp. 131-162. Oxford: Oxford University Press.
Dunin-Borkowski, O. M. and Brown, N. H. (1995). Mammalian CD2 is an effective heterologous marker of the cell surface in Drosophila. *Dev. Biol.* **168**, 689-693.
Genova, J. L., Jong, S., Camp, J. T. and Fehon, R. G. (2000). Functional analysis of Cdc42 in actin filament assembly, epithelial morphogenesis, and cell signaling during Drosophila development. *Dev. Biol.* **221**, 181-194.
Gisselbrecht, S., Skeath, J. B., Doe, C. Q. and Michelson, A. M. (1996). heartless encodes a fibroblast growth factor receptor (DFR1/DFGF-R2) involved in the directional migration of early mesodermal cells in the Drosophila embryo. *Genes Dev.* **10**, 3003-3017.
Gryzik, T. and Müller, H. A. (2004). FGF8-like1 and FGF8-like2 encode putative ligands of the FGF receptor Htl and are required for mesoderm migration in the Drosophila gastrula. *Curr. Biol.* **14**, 659-667.
Jannuzi, A. L., Bunch, T. A., Brabant, M. C., Miller, S. W., Mukai, L., Zavortink, M. and Brower, D. L. (2002). Disruption of C-terminal cytoplasmic domain of betaPS integrin subunit has dominant negative properties in developing Drosophila. *Mol. Biol. Cell* **13**, 1352-1365.
Jürgens, G., Wieschaus, E., Nüsslein-Volhard, C. and Kluding, H. (1984). Mutations affecting the pattern of the larval cuticle of Drosophila melanogaster. II. Zygotic loci on the third chromosome. *Rouxs Arch.* **193**, 283-295.
Kadam, S., McMahon, A., Tzou, P. and Stathopoulos, A. (2009). FGF ligands in Drosophila have distinct activities required to support cell migration and differentiation. *Development* **136**, 739-747.
Klingseisen, A., Clark, I. B., Gryzik, T. and Muller, H. A. (2009). Differential and overlapping functions of two closely related Drosophila FGF8-like growth factors in mesoderm development. *Development* **136**, 2393-2402.
Kölsch, V., Seher, T., Fernandez-Ballester, G. J., Serrano, L. and Leptin, M. (2007). Control of Drosophila gastrulation by apical localization of adherens junctions and RhoGEF2. *Science* **315**, 384-386.
Leptin, M. (1999). Gastrulation in Drosophila: the logic and the cellular mechanisms. *EMBO J.* **18**, 3187-3192.
Leptin, M. and Grunewald, B. (1990). Cell shape changes during gastrulation in Drosophila. *Development* **110**, 73-84.
Leptin, M., Bogaert, T., Lehmann, R. and Wilcox, M. (1989). The function of PS integrins during Drosophila embryogenesis. *Cell* **56**, 401-408.
Luo, L., Liao, Y. J., Jan, L. Y. and Jan, Y. N. (1994). Distinct morphogenetic functions of similar small GTPases: Drosophila Drac1 is involved in axonal outgrowth and myoblast fusion. *Genes Dev.* **8**, 1787-1802.
McMahon, A., Supatto, W., Fraser, S. E. and Stathopoulos, A. (2008). Dynamic analyses of Drosophila gastrulation provide insights into collective cell migration. *Science* **322**, 1546-1550.
McMahon, A., Reeves, G. T., Supatto, W. and Stathopoulos, A. (2010). Mesoderm migration in Drosophila is a multi-step process requiring FGF signaling and integrin activity. *Development* **137**, 2167-2175.
Millard, T. H. and Martin, P. (2008). Dynamic analysis of filopodial interactions during the zippering phase of Drosophila dorsal closure. *Development* **135**, 621-626.
Müller, H. A. (2008). Immunolabeling of embryos. *Methods Mol. Biol.* **420**, 207-218.
Murray, M. J. and Saint, R. (2007). Photoactivatable GFP resolves Drosophila mesoderm migration behaviour. *Development* **134**, 3975-3983.
Nieto, M. A., Sargent, M. G., Wilkinson, D. G. and Cooke, J. (1994). Control of cell behavior during vertebrate development by Slug, a zinc finger gene. *Science* **264**, 835-839.
Niewiadomska, P., Godt, D. and Tepass, U. (1999). DE-Cadherin is required for intercellular motility during Drosophila oogenesis. *J. Cell Biol.* **144**, 533-547.
Oda, H. and Tsukita, S. (1999). Dynamic features of adherens junctions during Drosophila embryonic epithelial morphogenesis revealed by a Dalpha-catenin-GFP fusion protein. *Dev. Genes Evol.* **209**, 218-225.
Oda, H., Tsukita, S. and Takeichi, M. (1998). Dynamic behavior of the cadherin-based cell-cell adhesion system during Drosophila gastrulation. *Dev. Biol.* **203**, 435-450.
Pacquelet, A. and Rorth, P. (2005). Regulatory mechanisms required for DE-cadherin function in cell migration and other types of adhesion. *J. Cell Biol.* **170**, 803-812.
Prasad, M. and Montell, D. J. (2007). Cellular and molecular mechanisms of border cell migration analyzed using time-lapse live-cell imaging. *Dev. Cell* **12**, 997-1005.
Schumacher, S., Gryzik, T., Tannebaum, S. and Müller, H. A. (2004). The RhoGEF Pebble is required for cell shape changes during cell migration triggered by the Drosophila FGF receptor Heartless. *Development* **131**, 2631-2640.
Shishido, E., Higashijima, S., Emori, Y. and Saigo, K. (1993). Two FGF-receptor homologues of Drosophila: one is expressed in mesodermal primordium in early embryos. *Development* **117**, 751-761.
Stathopoulos, A., Tam, B., Ronshaugen, M., Frasch, M. and Levine, M. (2004). pyramus and thisbe: FGF genes that pattern the mesoderm of Drosophila embryos. *Genes Dev.* **18**, 687-699.
Sun, X., Meyers, E. N., Lewandoski, M. and Martin, G. R. (1999). Targeted disruption of Fgf8 causes failure of cell migration in the gastrulating mouse embryo. *Genes Dev.* **13**, 1834-1846.
Tekotte, H., Tollervey, D. and Davis, I. (2007). Imaging the migrating border cell cluster in living Drosophila egg chambers. *Dev. Dyn.* **236**, 2818-2824.
Tepass, U., Gruszynski, D. E., Haag, T. A., Omatyar, L., Török, T. and Hartenstein, V. (1996). shotgun encodes Drosophila E-cadherin and is preferentially required during cell rearrangement in the neurectoderm and other morphogenetically active epithelia. *Genes Dev.* **10**, 672-685.
Thiery, J. P., Acloque, H., Huang, R. Y. and Nieto, M. A. (2009). Epithelial-mesenchymal transitions in development and disease. *Cell* **139**, 871-890.
van Impel, A., Schumacher, S., Draga, M., Herz, H.-M., Großhans, J. and Müller, H.A.-J. (2009). Regulation of the RacGTPase pathway by the multi-functional Rho GEF Pebble is essential for mesoderm migration in the *Drosophila* gastrula. *Development* **136**, 813-822.
Vincent, S., Wilson, R., Coelho, C., Affolter, M. and Leptin, M. (1998). The Drosophila protein Dof is specifically required for FGF signaling. *Mol. Cell* **2**, 515-525.
Weijer, C. J. (2009). Collective cell migration in development. *J. Cell Sci.* **122**, 3215-3223.
Wieschaus, E., Nüsslein-Volhard, C. and Jürgens, G. (1984). Mutations affecting the pattern of the larval cuticle in Drosophila melanogaster. III. Zygotic loci on the X chromosome and fourth chromosome. *Rouxs Arch* **193**, 296-307.
Wilson, R., Vogelsang, E. and Leptin, M. (2005). FGF signalling and the mechanism of mesoderm spreading in Drosophila embryos. *Development* **132**, 491-501.
Winklbauer, R. and Müller, H. A. (2011). Mesoderm layer formation in *Xenopus* and *Drosophila* gastrulation. *Phys. Biol.* (in press).
Winklbauer, R., Medina, A., Swain, R. K. and Steinbeisser, H. (2001). Frizzled-7 signalling controls tissue separation during Xenopus gastrulation. *Nature* **413**, 856-860.
Wright, T. R. (1960). The phenogenetics of the embryonic mutant, lethal myospheroid, in Drosophila melanogaster. *J. Exp. Zool.* **143**, 77-99.